1-1-2011

Comparison and Analysis of Empirical Equations For Soil Heat Flux for Different Cropping Systems and Irrigation Methods

A. Irmak
University of Nebraska-Lincoln, airmak2@unl.edu

R. K. Singh
USGS Earth Resources Observation and Science

Elizabeth A. Walter-Shea
University of Nebraska - Lincoln, ewalter-shea1@unl.edu

Shashi Verma
University of Nebraska - Lincoln, sverma1@unl.edu

Andrew E. Suyker
University of Nebraska - Lincoln, asuyker1@unl.edu

Comparison and Analysis of Empirical Equations for Soil Heat Flux for Different Cropping Systems and Irrigation Methods

A. Irmak, R. K. Singh, E. A. Walter-Shea, S. B. Verma, A. E. Suyker

Abstract. *We evaluated the performance of four models for estimating soil heat flux density (G) in maize (*Zea mays *L.) and soybean (*Glycine max *L.) fields under different irrigation methods (center-pivot irrigated fields at Mead, Nebraska, and subsurface drip irrigated field at Clay Center, Nebraska) and rainfed conditions at Mead. The model estimates were compared against measurements made during growing seasons of 2003, 2004, and 2005 at Mead and during 2005, 2006, and 2007 at Clay Center. We observed a strong relationship between the G and net radiation (R_n) ratio (G/R_n) and the normalized difference vegetation index (NDVI). When a significant portion of the ground was bare soil, G/R_n ranged from 0.15 to 0.30 and decreased with increasing NDVI. In contrast to the NDVI progression, the G/R_n ratio decreased with crop growth and development. The G/R_n ratio for subsurface drip irrigated crops was smaller than for the center-pivot irrigated crops. The seasonal average G was 13.1%, 15.2%, 10.9%, and 12.8% of R_n for irrigated maize, rainfed maize, irrigated soybean, and rainfed soybean, respectively. Statistical analyses of the performance of the four models showed a wide range of variation in G estimation. The root mean square error (RMSE) of predictions ranged from 15 to 81.3 W m^{-2}. Based on the wide range of RMSE, it is recommended that local calibration of the models should be carried out for remote estimation of soil heat flux.*

Keywords. *Energy balance, Maize, Remote sensing, Soybeans.*

Soil heat flux (G) plays an important role in land surface energy dynamics by constraining the amount of energy available for latent heat (LE) and sensible heat (H). It is a significant component of the daytime surface energy balance for almost all ecosystems, including deserts (Dugas et al., 1996). It can become a significant component in relatively sparse vegetation (Kustas et al., 2000) and predominant during night time (Murray and Verhoef, 2007a). An accurate quantification of G is of key importance in energy balance studies, particularly for energy balance closure assessment using eddy covariance (Stannard et al., 1994; Wilson et al., 2002; Shao et al., 2008) and Bowen ratio energy balance systems (BREBS), since BREBS require an estimate of available energy for computing evapotranspiration (ET). Malhi et al. (2004) suggested that errors in G estimation can be a possible explanation of the failure to close the energy budget. Accurately quantifying G is also important for energy balance-based model output verification (Heusinkveld et al., 2004; Murray and Verhoef, 2007a, 2007b).

Several vegetation indices, including normalized difference vegetation index (NDVI), have been correlated to G. The NDVI is computed using near-infrared (ρ_{NIR}) and red (ρ_R) band reflectance and a measure of vegetation amount and condition and is associated with biomass, leaf area index (LAI), and percentage of vegetation cover. Kustas and Daughtry (1990) developed a method for estimating G based on measurements of net radiation (R_n) and ground-based reflectance in bare soil, alfalfa (*Medicago sativa*), and cotton (*Gossypium hirsutum*) fields in Arizona during summer. They used a single-dome net radiometer with a polyethylene shield positioned about 1.5 m above the soil surface to measure R_n. The G was measured using three soil heat flux plates buried at a depth of 5 cm from the soil surface. A multiband radiometer (model 12-1000, Barnes Engineering Co., Stamford, Conn.), with filters to measure ground radiance in spectral bands matching the Landsat Thematic Mapper (TM), was used for reflectance measurement. The radiometer, with a 15° field of view, was mounted about 1.7 m above the soil surface. They developed two G/R_n equations based on the ratio of ρ_{NIR}/ρ_R and NDVI. The mid-day ratio of G and R_n (G/R_n) was linearly related to the ratio of ρ_{NIR}/ρ_R and NDVI. The NDVI was better correlated with the ratio of G/R_n as compared to the ρ_{NIR}/ρ_R ratio (r^2 = 0.86 vs. 0.74). Application of this method using remotely sensed multispectral data acquired from an aircraft over large agricultural fields in Arizona indicated that G was overestimated by 13% (Daughtry et al., 1990). However, the study was carried out at the same

Submitted for review in December 2008 as manuscript number SW 7834; approved for publication by the Soil & Water Division of ASABE in November 2010.

Contribution of the University of Nebraska-Lincoln, Agricultural Research Division, Lincoln, Nebraska. The mention of trade names or commercial products is solely for the information of the reader and does not constitute an endorsement or recommendation for use by the authors or the University of Nebraska-Lincoln.

The authors are **Ayse Irmak, ASABE Member Engineer,** Assistant Professor, School of Natural Resources Center for Advanced Land Management Information Technology (CALMIT) and Department of Civil Engineering, University of Nebraska-Lincoln, Lincoln, Nebraska; **Ramesh K. Singh, ASABE Member Engineer,** Scientist, USGS Earth Resources Observation and Science (EROS) Center, Sioux Falls, South Dakota; **Elizabeth A. Walter-Shea,** Professor, **Shashi B. Verma,** Professor, and **Andrew E. Suyker,** Assistant Professor, School of Natural Resources, University of Nebraska-Lincoln, Lincoln, Nebraska. **Corresponding author:** Ayse Irmak, 311 Hardin Hall, University of Nebraska-Lincoln, Lincoln, NE 68583-0973; phone: 402-472-8024; fax: 402-472-2946; e-mail: airmak2@unl.edu.

  ISSN 2151-0032

site using the datasets collected remotely during the experimental setup for model calibration.

Bastiaanssen et al. (1998) pooled G/R_n and NDVI data from Clothier et al. (1986), Choudhury (1989), Kustas and Daughtry (1990), and Van Oevelen (1991) to derive a G equation in the Surface Energy Balance Algorithm for Land (SEBAL) model. Melesse and Nangia (2005) ran the SEBAL model for ten Landsat Thematic Mapper (TM) and Enhanced Thematic Mapper (ETM) images in Montana. The Landsat images were acquired from 2001 to 2003, and the G equation in the SEBAL model was calibrated from data collected on grassland. They suggested a modified G equation that yielded a root mean square error (RMSE) of 10.5 W m^{-2} with 24.4% mean absolute percentage error between observed and predicted G. Singh et al. (2008) found that the soil heat flux used in the SEBAL model significantly overestimated G in a subsurface drip irrigated maize field in south-central Nebraska, with an r^2 of 0.055 and an RMSE of 79.8 W m^{-2}. The poor estimates of G could be attributed to the fact that the surface soil in a subsurface drip irrigated field is very dry for the majority of the growing season, and there is no surface evaporation due to irrigation. These conditions may be considerably different from those in which the G equations were derived. In such conditions, evaporative cooling in the topsoil is reduced due to reduced soil evaporation, which results in increased soil temperature and increased G. However, since the surface is usually dry, there is less heat exchange with the surface, and thus less magnitude of heat flux can be expected than the rate estimated by SEBAL. Singh et al. (2008) used measured G data to develop an exponential relation that utilizes NDVI and R_n, which resulted in an r^2 of 0.74 and RMSE of 20.1 W m^{-2}.

Our overall objective was to apply and test the aforementioned empirical equations (Kustas and Daughtry, 1990; Bastiaanssen et al., 1998; Melesse and Nangia, 2005; Singh et al., 2008) to estimate G under maize (*Zea mays* L.) and soybean (*Glycine max* L.) cropping systems in Nebraska soil and climatic conditions. Specific objectives were to (1) investigate seasonal and inter-annual progression of the G/R_n ratio and NDVI to understand how G/R_n dynamics respond to changes in soil, climate, land use, and management conditions for maize and soybean cropping systems; and (2) evaluate the ability of the aforementioned equations to predict soil heat flux under the aforementioned conditions.

Materials and Methods

Measured Rn and NDVI Based Soil Heat Flux Equations

Four existing empirical equations were evaluated for their ability to estimate G as a function of R_n and NDVI: Kustas and Daughtry (1990), Bastiaanssen et al. (1998), Melesse and Nangia (2005), and Singh et al. (2008). NDVI is computed using near-infrared (ρ_{NIR}) and red (ρ_R) band reflectance, as proposed by Rouse et al. (1973):

$$\mathrm{NDVI} = \frac{\rho_{NIR} - \rho_R}{\rho_{NIR} + \rho_R} \quad (1)$$

Kustas and Daughtry (1990) developed two equations from the same dataset:

$$\frac{G}{R_n} = 0.294 - 0.0164\frac{\rho_{NIR}}{\rho_R} \quad (r^2 = 0.74,\ n = 11) \quad (2)$$

$$\frac{G}{R_n} = 0.325 - 0.208\,\mathrm{NDVI} \quad (r^2 = 0.86,\ n = 11) \quad (3)$$

Equation 3 is used in our analysis, since G is computed as a function of NDVI. Equation 3 indicates that with full canopy cover (NDVI ~ 1) about 12% of R_n is used to heat the soil, and under bare soil conditions (NDVI ~ 0) G can be as much as 32% of R_n.

Bastiaanssen et al. (1998) developed the following equation to estimate G in the SEBAL model:

$$\frac{G}{R_n} = 0.30\,(1 - 0.98\,\mathrm{NDVI}^4) \quad (r^2 = 0.61,\ n = 35) \quad (4)$$

Equation 4 implies that G can be as little as 0.6% of R_n when the ground has full canopy cover (NDVI ~ 1) and as much as 30% of R_n for bare soils (NDVI ~ 0).

Melesse and Nangia (2005) calibrated equation 4 in the SEBAL model with data collected on grassland in Montana and suggested equation 5 for G:

$$\frac{G}{R_n} = 0.153\,(1 - 0.98\,\mathrm{NDVI}^4) \quad (5)$$

The calibration by Melesse and Nangia (2005) resulted in a smaller offset value (0.15) than equation 4 (0.30). Thus, equation 5 yields 50% smaller G values than equation 4 under similar ground cover conditions. Singh et al. (2008) developed the following equation using data from a subsurface drip irrigated maize field (Irmak and Irmak, 2008):

$$G = [0.3811\exp(-2.3187\,NDVI)]R_n \quad (6)$$

Equation 6 will likely produce a higher rate of G under bare soil (NDVI ~ 0) than the above equations (i.e., offset is 0.38).

Two different existing datasets were used to evaluate equation 3 (model 1 or M1), equation 4 (model 2 or M2), equation 5 (model 3 or M3), and equation 6 (model 4 or M4). The first dataset was from an ongoing carbon sequestration program (CSP) representing three major cropping systems at Mead, Nebraska. The second dataset was from the South Central Agricultural Laboratory (SCAL) of the University of Nebraska-Lincoln, near Clay Center, Nebraska.

Study Site, Equipment, and Experimental Procedures at Mead, Nebraska

We used datasets collected by Verma et al. (2005) and Suyker et al. (2005) at three sites near Mead, Nebraska, during 2003 to 2005 as part of an ongoing carbon sequestration research program at the University of Nebraska-Lincoln Agricultural Research and Development Center (ARDC) in Ithaca, Nebraska. Figure 1 shows average weather conditions at the site from a nearby High Plains Regional Climate Center (HPRCC) automated weather station (www.hprcc.unl.edu). The datasets measured at the HPRCC stations included daily maximum and minimum temperature (T_{max} and T_{min}), relative humidity, wind speed, and solar radiation. The study sites at the ARDC represent three major cropping systems: irrigated continuous maize, irrigated maize-soybean rotation, and rainfed maize-soybean rotation. The first site (site 1)

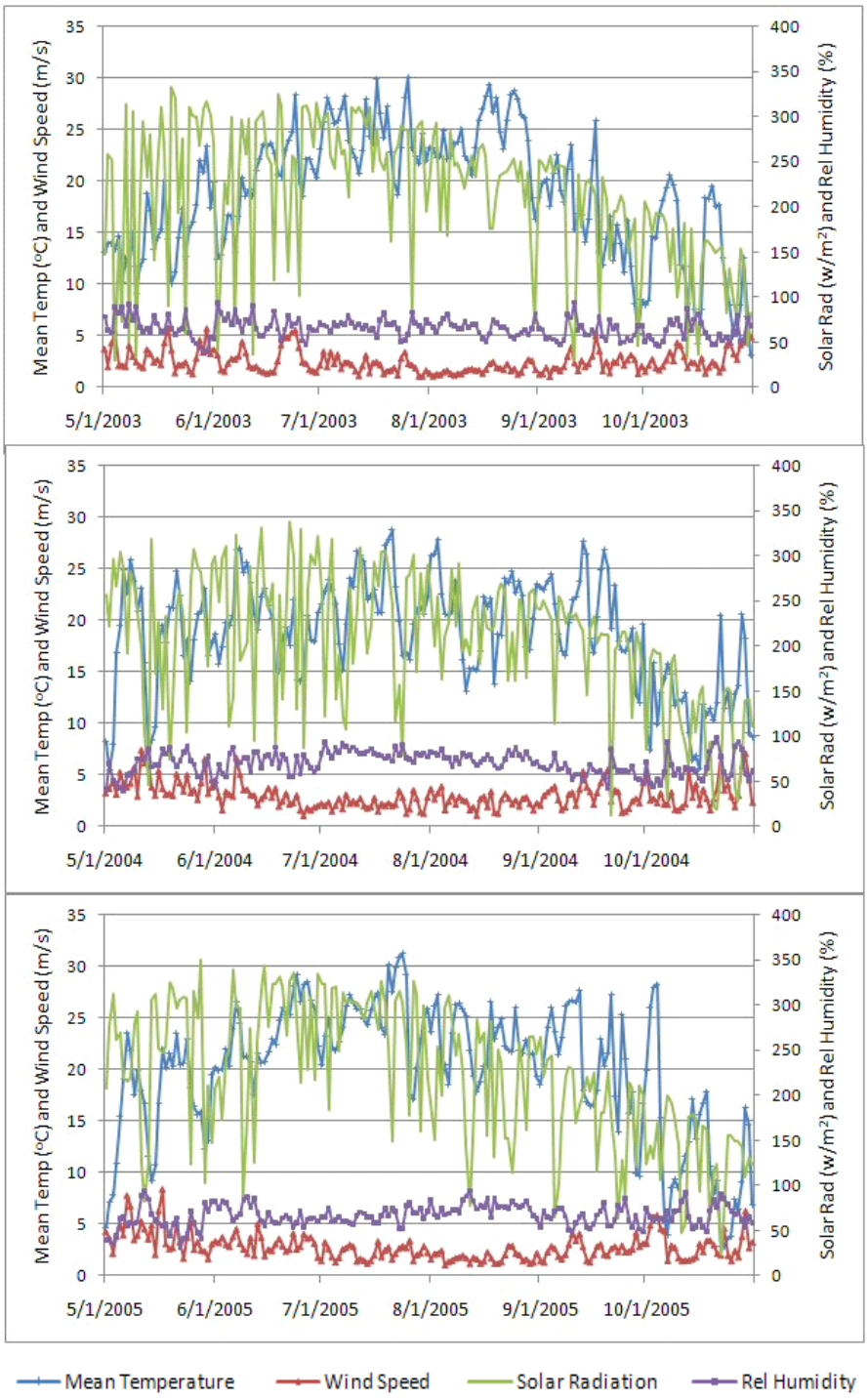

Figure 1. Daily climate variables including mean temperature (°C), wind speed (m s^{-1}), solar radiation (W m^{-2}), and relative humidity (%) during three crop growing seasons at the Mead study sites for 2003, 2004, and 2005.

(41° 9′ 54.2″ N, 96° 28′ 35.9″ W, 361 m above mean sea level) is irrigated with a center-pivot irrigation system and is about 48.7 ha in size. The second site (site 2) (41° 9′ 53.5″ N, 96° 28′ 12.3″ W, 362 m above mean sea level) is also center-pivot irrigated and is 52.4 ha in size, and the third site (site 3) (41° 10′ 46.8″ N, 96° 26′ 22.7″ W, 362 m above mean sea level) is rainfed and about 65.4 ha in size. These three sites are within 1.6 km of each other. All three sites are large enough to provide sufficient upwind fetch of uniform cover for energy flux measurements using eddy covariance systems. Since the beginning of the study in 2001, all these sites have been under no-till conditions. Prior to initiation of the study, sites 1 and 2 had a 10-year history of maize-soybean rotation under no-till. Site 3 had a history of variable cropping practices of primarily wheat, soybean, oats, and maize grown in 2 to 4 ha plots with tillage. All three sites were uniformly tilled by disking prior to initiation of the study to homogenize the top 0.10 m of soil and to incorporate P and K fertilizers, as well as previously accumulated surface residues.

Table 1. Cropping details of the study sites, including plat population, planting date, and harvest date.

Site	Year	Crop (Cultivar)	Plant Population (plants ha^{-1})	Planting Date	Harvest Date
Mead site 1: Irrigated, continuous maize	2003	Maize (Pioneer 33B51)	77,000	May 15	October 27
	2004	Maize (Pioneer 33B51)	79,800	May 3	October 13
	2005	Maize (DeKalb 63-75)	69,200	May 4	October 12
Mead site 2: Irrigated, maize-soybean rotation	2003	Maize (Pioneer 33B51)	78,000	May 14	October 23
	2004	Soybean (Pioneer 93B09)	296,000	June 2	October 18
	2005	Maize (Pioneer 33B51)	76,300	May 2	October 17
Mead site 3: Rainfed, maize-soybean rotation	2003	Maize (Pioneer 33B51)	57,600	May 13	October 13
	2004	Soybean (Pioneer 93B09)	264,700	June 2	October 11
	2005	Maize (Pioneer 33G66)	53,700	April 26	October 17
Clay Center: Subsurface drip irrigated	2005	Maize (Pioneer 33B51)	72,900	April 22	October 17
	2006	Maize (Pioneer 33B54)	75,400	May 12	October 5-6
	2007	Soybean (Pioneer 93M11)	385,500	May 21	October 24

The soils at all three sites are deep silty clay loams consisting of four soil series: Yutan (fine-silty, mixed, superactive, mesic Mollic Hapludalfs); Tomek (fine, smectitic, mesic Pachic Argiudolls); Filbert (fine, smectitic, mesic Vertic Argialbolls); and Fillmore (fine, smectitic, mesic Vertic Argialbolls). The general particle size distribution is 13% sand, 57% silt, 27.5% clay, and 2.5% organic matter with a field capacity of 0.32 m^3 m^{-3} and permanent wilting point of 0.19 m^3 m^{-3}. The cropping details of the sites are presented in table 1. Maize was planted at site 1 during the three study years (2003, 2004, and 2005). At site 2, maize was planted in 2003 and 2005, whereas soybean was planted in 2004. Similarly, at the rainfed site 3, maize was planted in 2003 and 2005, and soybean was planted in 2004. The amounts of irrigation applied at site 1 were 378, 260, and 324 mm in 2003, 2004, and 2005, respectively. The amounts of irrigation provided at site 2 during 2003, 2004 and 2005 were 350, 184, and 309 mm, respectively. More details about these sites and the experimental setup can be found in Verma et al. (2005) and Suyker et al. (2005).

Net radiation was measured at 5.5 m above the ground using a Kipp & Zonen CNR1 net radiometer (Campbell Scientific Inc., Logan, Utah). The net radiometer consists of one pair of pyranometers and pyrgeometers. The incoming and outgoing shortwave radiation (0.3 to 2.8 μm) was measured by the pyranometers, while the upwelling and downwelling far-infrared radiation (5 to 50 μm) were measured by the pyrgeometers. The typical response time of the instrument was about 18 s, and the operating temperature range was -40°C to 70°C. Soil heat flux was measured at a depth of 0.06 m below the soil surface using two soil heat flux plates (Radiation and Energy Balance Systems, Inc., Seattle, Wash.) on either side of the crop row. The soil heat flux was adjusted for soil moisture variation (Verma et al., 2005). Net radiation and soil heat flux were sampled at 8 s intervals and averaged over 60 min using a CR10X datalogger and AM416 relay multiplexer (Campbell Scientific, Inc., Logan, Utah).

Spectral reflectance was measured in 2003, 2004, and 2005 with a pair of inter-calibrated four-channel light sensors (model SKR 1850, Skye Instruments, Ltd., Powys, U.K.) mounted at approximately 5 m on a mast located near the eddy covariance flux tower in the center of the fields. One radiometer measured downwelling irradiance ($E\lambda_{inc}$), and the other measured upwelling radiance ($L\lambda_{canopy}$). The upward-directed radiometer was equipped with a cosine diffuser to give a hemispherical view of the incoming radiation, while the downward (nadir)-facing sensor had a 25° field of view, providing a footprint of approximately 3.86 m^2 at ground level. The Skye radiometers measure in four narrow spectral bands: 536-561 nm (green band), 665-676 nm (red band), 700-720 nm (red-edge band) and 862-874 nm (near-infrared band); all bands except the 700-720 nm red-edge band are comparable to Moderate Resolution Imaging Radiometer (MODIS) bands. The upwelling and downwelling radiometers were inter-calibrated to match their transfer functions by measuring the upwelling radiance of an illuminated Spectralon reflectance standard ($L\lambda_{ref}$; Labsphere, North Sutton, N.H.) simultaneously with incident irradiance ($E\lambda_{ref}$) from the upward-directed spectrometer before and after the study period (April-May and October-November). Using a field goniometer system (Walter-Shea et al., 1993), the relation of the transfer functions under varying solar zenith angles between the upwelling radiance from the reflectance standard ($L\lambda_{cal}$) and the downwelling irradiance ($E\lambda_{cal}$) was quantified. Little change in the pre- and post- measurements confirmed the stability of the instruments. The reflectance standard was corrected for anisotropic reflectance ($\rho_{\lambda ref}$; Jackson et al., 1987). Percent spectral reflectance ($\rho\lambda$) was calculated as:

$$\rho_\lambda = \frac{L_{\lambda canopy}}{E_{\lambda inc}} \frac{E_{\lambda ref}}{L_{\lambda ref}} \rho_{\lambda ref} 100 \quad (7)$$

In the field, the Skye radiometers measured the same location, obtaining a 10 min average every half-hour between 11:30 a.m. and 1:30 p.m. (Central Standard Time, CST), with solar zenith angles ranging from approximately 18° to approximately 50° depending on the time of the year.

Study Site, Equipment, and Experimental Procedures at Clay Center, Nebraska

We used three years of data collected during 2005, 2006, and 2007 from an experimental field at the University of Nebraska-Lincoln South Central Agricultural Laboratory (SCAL) at Clay Center, Nebraska. The datasets from this site are part of an ongoing extensive field campaign that is designed to measure surface energy fluxes, soil moisture, and plant physiological parameters and their relations with microclimatic variables for various surfaces (Irmak, 2010). The data collection campaign is part of the Nebraska Water and Energy Flux Measurement, Modeling, and Research Network (NEBFLUX) that operates ten Bowen Ratio Energy

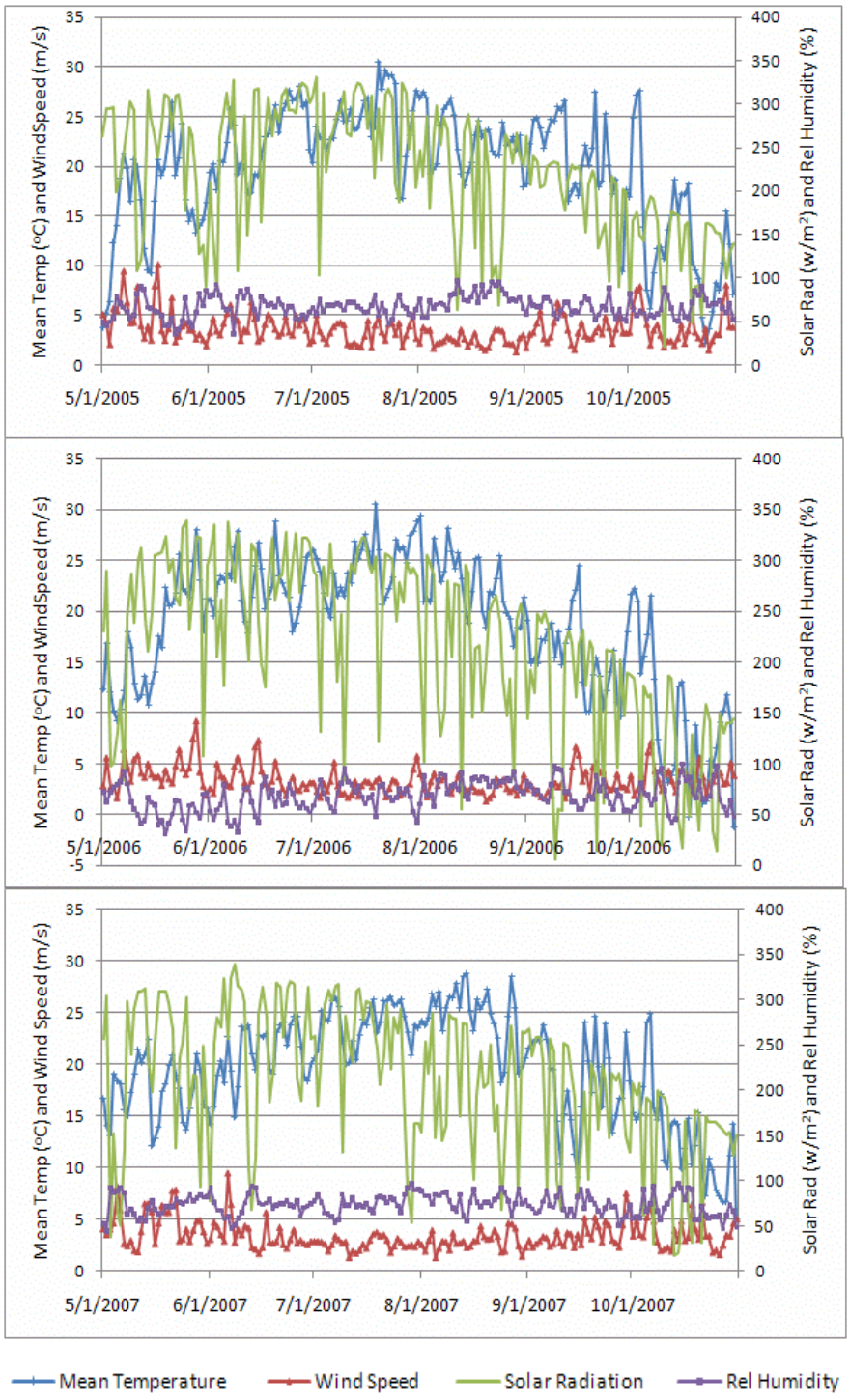

Figure 2. Daily climate variables including mean temperature (°C), wind speed (m s^{-1}), solar radiation (W m^{-2}), and relative humidity (%) during three crop growing seasons at the Clay Center study site for 2005, 2006, and 2007.

Balance Systems (BREBS) and one eddy covariance system over various vegetation surfaces ranging from irrigated and rainfed grasslands, to tilled and untilled and irrigated and rainfed croplands, to Phragmites (*Phragmites australis*)-dominated cottonwood (*Populus deltoides* var. *occidentalis*) and willow stand (*Willow salix*) plant communities. Experimental details are provided by Irmak et al. (2008), Irmak and Mutiibwa (2009a, 2009b), Irmak and Mutiibwa (2010), and Irmak (2010).

The SCAL is located approximately 160 km west of Lincoln in the south-central part of Nebraska (40° 34′ N, 98° 8′ W, 552 m above sea level). The experimental field at SCAL was 13 ha in size and was irrigated using a subsurface drip irrigation system that was installed in 2004. The drip laterals were spaced every 1.52 m (every other maize row) in the middle of the row and were installed at a depth of approximately 0.40 m below the soil surface. The soil at the field is a Hastings silt loam, which is a well-drained soil on uplands (fine, montmorillonitic, mesic Udic Argiustoll) with a field

moisture capacity of 0.34 m^3 m^{-3} and permanent wilting point of 0.14 m^3 m^{-3}. The particle size distribution is 15% sand, 62.5% silt, 20% clay, and 2.5% organic matter content. The daily meteorological conditions for the 2005, 2006, and 2007 growing seasons from the nearby HPRCC weather station are presented in figure 2. The prevailing wind direction at the experimental site is south-southwest.

Maize was planted on April 22 and May 12 during the 2005 and 2006, respectively (table 1). The field was harvested on October 17 in 2005 and on October 5-6 in 2006. Soybean was planted on May 21 and harvested on October 24 in 2007. This field was planted to rainfed maize in the previous four years. Irrigations were applied two or three times a week to replenish the soil water content to approximately 90% of field capacity in the effective root zone depth.

A BREBS was installed in the field in 2005 with a fetch distance of 520 m in the north-south direction and 280 m in the east-west direction. One of the main advantages of the BREBS over other systems (i.e., eddy covariance system, ECS) is that it does not require forcing the energy balance equation for closure, as is the case with the ECS. The BREBS may not require as much fetch as ECS. However, the BREBS assumes that the diffusivity for heat and water vapor is equal, which may not be the case for all surfaces. Furthermore, in the BREBS theory, when the Bowen ratio is close to -1 (i.e., $\beta \sim -1$), the measured latent heat values may become unstable. Although this condition ($\beta \sim -1$) may occur only for a very limited time when the latent heat is very small (i.e., late night or very early in the morning), alternative techniques can be used to easily overcome this issue with the BREBS. Here we provide a brief description of soil heat flux and other surface energy flux measurements and crop and soil management practices. Detailed descriptions of the microclimate measurements, including latent heat flux, sensible heat, soil heat flux, net radiation, and other microclimatic variables (vapor pressure, air temperature, relative humidity, wind speed and direction, incoming and outgoing shortwave radiation, albedo, and soil temperature) are presented by Irmak (2010) and in the aforementioned studies.

Measurements were made using a deluxe version of a BREBS (Radiation and Energy Balance Systems, REBS, Inc., Bellevue, Wash.). Chromel-constantan thermocouple probes were used to measure temperature and humidity gradients (model THP04015 for temperature and THP04016 for humidity, REBS, Inc., Bellevue, Wash.) with a resolution of 0.0055°C for temperature and 0.033% for humidity. The deluxe BREBS used an automatic exchange mechanism that physically exchanged the temperature and humidity sensors at two heights above the canopy. Soil heat flux was measured using three REBS HFT-3.1 heat flux plates and three soil thermocouples. Each soil heat flux plate was placed at a depth of approximately 0.06 m below the mean ground level. The REBS STP-1 soil thermocouple probes were installed in close proximity to each soil heat flux plate at depths of 0.02, 0.04, 0.06, 0.08, and 0.10 m below the soil surface. Measured soil heat flux values were adjusted to soil temperatures and soil water content, as measured using three REBS SMP1R soil moisture probes. One soil moisture probe was installed in close proximity to each soil heat flux plate. The SMP1R probes were installed at 0.06 m below the surface and approximately 0.20 m away from the heat flux plate to adjust the soil heat flux for the soil water content. Soil heat flux plates were installed on the crop row, on the row where the drip lateral (tape) was installed (the drip lateral was installed 0.40 m below the surface every other furrow), and on the row without drip lateral. Since the net radiometer measures the net radiation from all these three cases, the average of all soil heat flux plates was used in the analyses. Net radiation was measured using a REBS Q*7.1 net radiometer that was installed approximately 4.5 m above the soil surface. The radiometer was sensitive to wavelengths from 0.25 to 60 μm. The net radiometer was attached to a 5 m long metal arm to extend the radiometer away from the tripod (horizontally to the crop canopy) so that the reflection of heat and radiation from any instrument was eliminated. The radiometer consists of two chromel-constantan (type E) differential thermocouple junctions that are installed to monitor temperature differences between the core and the upper and lower windshields (domes). The net radiometer was supplied with a constant airflow through a desiccant tube to keep air space inside the dome dry. All variables were sampled at 60 s intervals and averaged and recorded on an hourly basis using a CR10X datalogger and AM416 relay multiplexer (Campbell Scientific, Inc., Logan, Utah). All system components were powered by a solar panel and a 12 V, 140 A marine battery. The BREBS data were downloaded from the datalogger on a weekly basis and carefully screened for quality control (Irmak and Irmak, 2008; Irmak and Mutiibwa, 2009a, 2009b; Irmak, 2010).

The NDVI at the Clay Center site was calculated using cloud-free Landsat 5 and Landsat 7 satellite images (path 29, row 32). Seven images were used for each of the 2005 and 2006 growing seasons, and five images were used for the 2007 growing season (table 2). The digital numbers (DN) of the images were converted to radiance and then to reflectance using modified parameters (Chander and Markham, 2003) in ERDAS Imagine software (Leica Geosystems Geospatial Imaging, Norcross, Ga.). The NDVI was computed using near-infrared (band 4) and red (band 3) reflectance using equation 1.

Table 2. Details of Landsat images (path 29, row 32) used for the study.

Image Acquisition			
Year	Date	DOY	Satellite/Sensor
2005	May 19	139	L5/TM
	June 20	171	L5/TM
	July 22	203	L5/TM
	August 07	219	L5/TM
	September 08	251	L5/TM
	September 16	259	L7/ETM
	October 18	291	L7/ETM
2006	May 22	142	L5/TM
	June 23	174	L5/TM
	July 17	198	L7/ETM
	July 25	206	L5/TM
	September 19	262	L7/ETM
	October 13	286	L5/TM
	October 29	302	L5/TM
2007	June 10	161	L5/TM
	July 12	193	L5/TM
	August 13	225	L5/TM
	September 22	265	L7/ETM
	September 30	273	L5/TM

Statistical Analysis

The performances of the four models for estimation of G were compared using various statistical measures, including mean absolute error (MAE, W m^{-2}), root mean square error (RMSE, W m^{-2}), coefficient of determination (r^2), index of agreement (d), and percentage error (PE), as shown in equations 8 through 12:

$$\text{MAE} = \sum_{i=1}^{n} \frac{|P_i - O_i|}{n} \tag{8}$$

$$\text{RMSE} = \sqrt{\frac{1}{n}\sum_{i=1}^{n}(P_i - O_i)^2} \tag{9}$$

$$r^2 = \left[\frac{\sum_{i=1}^{n}(O_i - \overline{O})(P_i - \overline{P})}{\sqrt{\sum_{i=1}^{n}(P_i - \overline{P})^2 \sum_{i=1}^{n}(O_i - \overline{O})^2}} \right]^2 \tag{10}$$

$$d = 1 - \frac{\sum_{i=1}^{n}(O_i - P_i)^2}{\sum_{i=1}^{n}\left(|P_i - \overline{O}| + |O_i - \overline{O}| \right)^2} \tag{11}$$

$$\text{PE} = \frac{\text{MAE (or RMSE)}}{G_{mean}} 100 \tag{12}$$

where P_i and O_i are the ith predicted and observed values, respectively; $\overline{P}$ and $\overline{O}$ are the average of n number of predicted and observed values, respectively; and G_{mean} is the seasonal average soil heat flux calculated for each year using the midday G measurements from May through end of October at each site.

A model with low MAE and RMSE is considered a better fit. Although r^2 has been widely used for model evaluation, it has been shown that r^2 is oversensitive to outliers and insensitive to additives (Legates and McCabe, 1999). The r^2 ranges from 0 to 1, with higher values indicating lower error variance. The index of agreement (d) was proposed by Willmot (1981) to overcome the insensitivities of r^2 and the Nash-Sutcliffe coefficient of efficiency (Moriasi et al., 2007) to differences in the observed and predicted means and variances (Legates and McCabe, 1999). The index of agreement (d) represents the ratio of the mean square error and the potential error (Willmot, 1984). The potential error in the denominator represents the largest value that the squared difference of each pair can attain. The range of d is similar to that of r^2 and lies between 0 (no correlation) and 1 (perfect fit).

The percentage error (PE) of MAE and RMSE is calculated based on mean measured G. In general, soil heat flux is a small portion of daily energy balance. However, on an hourly or shorter time step, G can have a considerable contribution to the energy balance. Given the fact that G varies considerably from one location to another in the field, as a function of various factors, and that its prediction is difficult, we assumed that ±30% deviation from the mean measured G would be an acceptable PE when evaluating model performance.

Results and Discussion

Seasonal Progression of G/Rn and NDVI for Irrigated and Rainfed Maize in Relation to Crop Growth and Development

The total amount of precipitation during the growing season (May 1 to Oct. 31) at Mead was 370, 409, and 330 mm for 2003, 2004, and 2005, respectively (fig. 3). The normal precipitation at this site for the growing season is about 510 mm. Year 2004 was very dry from mid-July to mid-August with little precipitation, while precipitation was plentiful in the early and late growing season. Fields at this site received more precipitation after day of year (DOY) 250 in 2004 than in 2003 and 2005. The precipitation pattern in 2003 was similar to 2005 except that most of the precipitation occurred in the beginning of the season (DOY 125-170).

The progression of the measured G/R_n ratio at 12:30 p.m. (CST) and NDVI for the irrigated continuous maize experiment (site 1) at Mead is presented in figure 4. We excluded questionable data from the figures and analysis due to instrument malfunction and rainfall events at the Mead sites. Therefore, data are missing for different periods in figure 4, 5, 7, 8, 9, and 10. The G/R_n ratio was high when a significant portion of the ground was bare soil, ranging from 0.15 to 0.30, and decreased with increasing NDVI (fig. 4a). Similar results were found for all three years at site 1. The NDVI increased gradually during the maize vegetative development stage and reached its maximum value within two months after planting (tasseling). It remained fairly constant during the reproductive stage and decreased gradually after plants reached physiological maturity. At Mead site 1 during 2003, NDVI started to increase 17 days after planting (DAP), reached its maximum value (0.89) by 62 DAP, and remained fairly constant until 97 DAP (fig. 4a). Thereafter, NDVI decreased gradually with crop senescence and continued to decrease until the harvest on 165 DAP. In contrast to NDVI progression, the G/R_n ratio decreased with crop growth and development. This decrease in G/R_n was due to the increase in ground cover. Higher ground cover, as indicated by higher NDVI, acts as a barrier to the transmission of solar radiation to the soil surface so that less R_n is consumed in heating of the soil. The G/R_n ratio continued to decrease even after the NDVI had reached its maxima (figs. 4a to 4c). This was due to the saturation of NDVI after reaching a certain leaf area index (LAI). Previous

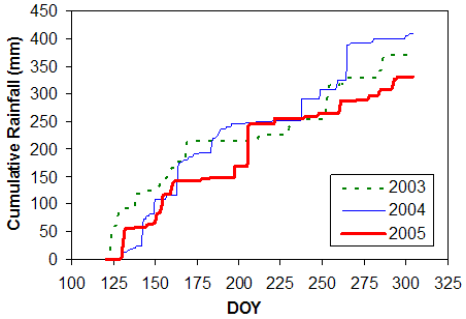

Figure 3. Cumulative precipitation at the Mead study sites (sites 1, 2, and 3) for the period of May 1 to October 31 during 2003, 2004, and 2005.

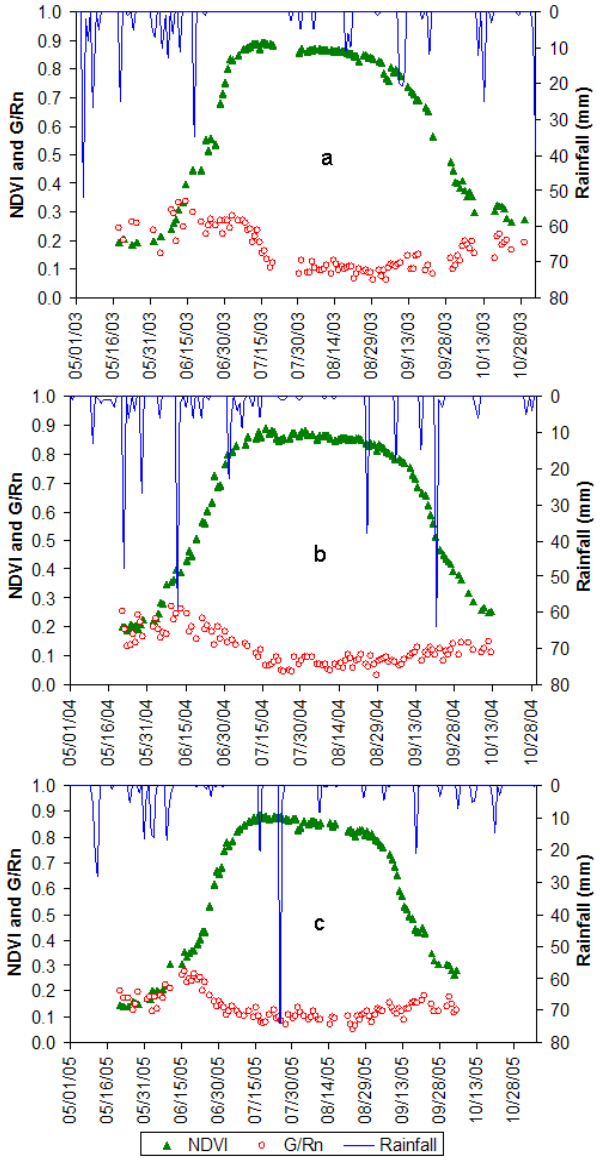

Figure 4. Seasonal progression of G/R_n and NDVI for irrigated maize at Mead site 1 (continuous maize) during the crop growing seasons in (a) 2003, (b) 2004, and (c) 2005. Daily precipitation is also shown in the graphs.

studies have shown that NDVI saturates once the LAI reaches a certain threshold value; beyond this threshold, LAI can increase while NDVI remains constant (Neale et al., 1989; Gitelson et al., 2003; Vina et al., 2004). Maize NDVI reaches its maxima at an LAI of approximately 3.0 (Neale et al., 1989). In our case, G/R_n reached its lowest value of about 0.10 by 75 DAP, indicating peak LAI of the crop by that time.

Results indicated that early NDVI at site 1 during 2005 was lower (0.15 vs. 0.20) as compared with the values obtained in 2003 and 2004 (fig. 4c). This may be due to the lower plant population in 2005 (69,200 plants ha^{-1}) as compared to 2003 (77,000 plants ha^{-1}) and 2004 (79,800 plants ha^{-1}). It is also possible that crop growth may have been poor in the beginning of the season due to low precipitation during the first 50 DAP. Although site 1 was irrigated, the first irrigation was not applied until 51 DAP. The maximum NDVI (0.88) was reached by 74 DAP and decreased to about 0.81 by 116 DAP.

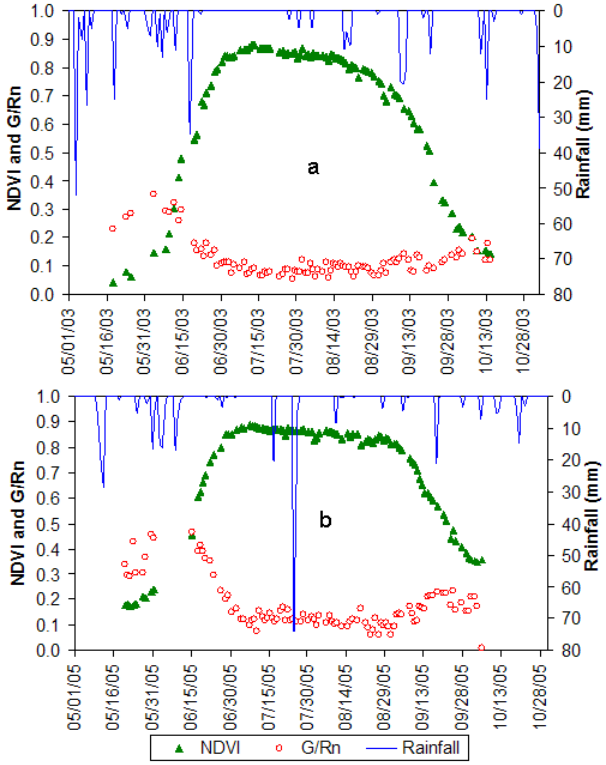

Figure 5. Seasonal progression of G/R_n and NDVI for irrigated maize at Mead site 2 (maize-soybean rotation) during the crop growing seasons in (a) 2003 and (b) 2005. Daily precipitation is also shown in the graphs.

The pattern of NDVI and G/R_n variation was similar in 2003 and 2005 at site 2 (fig. 5). However, the G/R_n values for 2003 and 2005 at site 2 (fig. 5) were slightly higher than the corresponding values at site 1 during the maize vegetative development stage (fig. 4). For instance, the G/R_n ratio at site 2 varied from 0.25 to 0.45 early in the growing season in 2003 and 2005, indicating that as much as 20% or more of R_n was stored in the ground at site 2 as compared to site 1. The crops at both sites were planted within one or two days, and the difference in G/R_n was probably due to differences in crop rotation practices (all sites were under no-till management during 2003-2005). Site 2 has a maize-soybean rotation, resulting in lesser amounts of crop residue produced as compared to the crop residue from the continuous maize practice at site 1. Therefore, the G/R_n ratio is higher, especially in year 2005, than in 2003 at site 2.

During 2003, the maximum NDVI (0.88) was observed by 59 DAP with a corresponding G/R_n value of 0.09 (fig. 5a). The G/R_n ratio remained fairly constant (~0.08 to 0.10) during the mid-growing season in 2003. The NDVI decreased to about 0.80 by 100 DAP. As compared to the crop at site 2 in 2003, there was delayed maturity of the crop in 2005 (fig. 5b). The NDVI started decreasing by 100 DAP in 2003, whereas it started decreasing by about 116 DAP in 2005.

The NDVI at the Clay Center site was obtained using Landsat 5 and Landsat 7 images from only cloud-free days of satellite overpasses during the growing seasons. The trend of NDVI was similar during 2005 and 2006 except during the late growing season (fig. 6). The maximum observed NDVI was 0.76 on 91 DAP in 2005 and on 66 DAP in 2006. After reaching the maximum NDVI, there was a sharp decrease in NDVI during 2006 as compared to 2005, indicating earlier

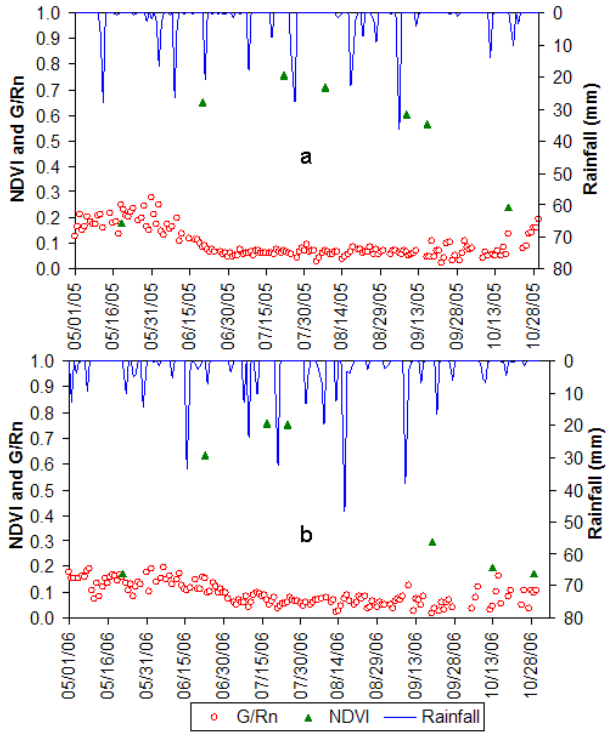

Figure 6. Seasonal progression of G/R_n and NDVI for irrigated maize at the Clay Center site during the crop growing seasons in (a) 2005 and (b) 2006. Daily precipitation is also shown in the graphs.

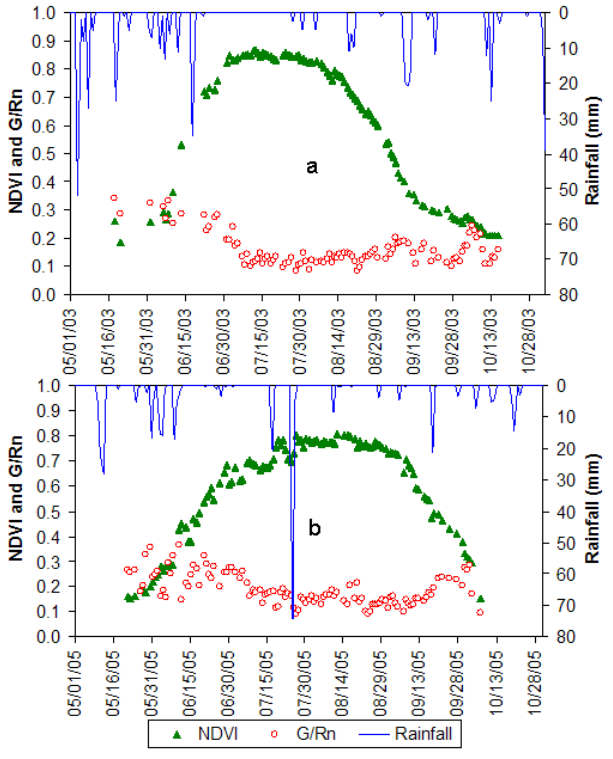

Figure 7. Seasonal progression of G/R_n and NDVI for rainfed maize at Mead site 3 (maize-soybean rotation) during the crop growing seasons in (a) 2003 and (b) 2005. Daily precipitation is also shown in the graphs.

maturity of the crop. The midday G/R_n ratio shows that G was in the range of 6% to 7% of R_n during the mid-growing season in 2005 and 2006 (fig. 6). The G/R_n ratio at Clay Center was smaller than at the irrigated sites (sites 1 and 2) at Mead.

The maximum NDVI of maize at Mead rainfed site 3 during 2003 was slightly lower 0.86 (fig. 7a) than the maximum values at irrigated site 1 (0.89) and site 2 (0.88) during the same year. Based on the field sampling from 20 different fields in south-central Nebraska, it has been shown that irrigated crops have higher mean NDVI than rainfed fields (Singh and Irmak, 2009). The well-irrigated, healthy green vegetation has more ground cover and produces more chlorophyll, resulting in more absorption of red light and higher NDVI.

The crop at Mead site 3 reached maturity about a week earlier than at irrigated sites 1 and 2 during 2003 (figs. 4, 5, and 7). With crop senescence, NDVI decreased to about 0.80 by 87 DAP and then decreased sharply until the harvest on October 13, 2003. The G/R_n ratio during the early growing season was in the range of 0.25 to 0.35 but started decreasing with increasing NDVI from 19 DAP. By 56 DAP, G/R_n reached about 0.10 and remained fairly constant in the range of 0.10 to 0.15 during the mid-growing season (fig. 7a).

In 2005, maize was planted on April 26 at Mead site 3, about a week earlier than at site 1 (May 4) and site 2 (May 2). The NDVI reached its maximum value of 0.80 by 91 DAP and remained relatively constant (0.78 to 0.80) until 116 DAP (fig. 7b). The G/R_n ratio was scattered in the range of 0.15 to 0.35 during the early growing season in 2005 and decreased only after 66 DAP (fig. 7b). Site 3 at Mead had the lowest plant population (53,700 plants ha^{-1}) during 2005 among all the maize sites, which resulted in higher radiation penetration into the canopy and soil surface, resulting in higher G toward the soil.

Seasonal Progression of G/Rn and NDVI for Irrigated and Rainfed Soybean

The seasonal progression of G/R_n and NDVI of the irrigated soybean crop at Mead site 2 during 2004 is shown in figure 8. The G/R_n ratio varied from 0.10 to 0.21 during the early growth stage in 2004 and was smaller than the value (0.25 to 0.45) at site 2 for maize in 2003. This was due to the presence of greater crop residue in 2004 from the previous year. Maize and soybean residues and the soil (at different moisture content) have different reflectance properties. Some of the differences in G/R_n are related to differences in crop residue type and amount. For instance, maize following soybean is likely to have higher G due to the lower amount of crop residue from the previous year's soybean crop.

The temporal distribution of G/R_n and NDVI for the soybean crop during 2007 at Clay Center is presented in figure 9. The G/R_n ratio on 20 DAP was 0.28, which decreased to 0.08 by 84 DAP. The maximum NDVI (0.78) was observed on 81 DAP. Thereafter, NDVI decreased with the increase in G/R_n. Since we had only five Landsat images for the 2007 growing season, it is possible that we might have missed some extreme values of NDVI and G/R_n. The maximum NDVI of soybean was slightly higher than the maximum NDVI of maize both at Clay Center and Mead.

Under the rainfed maize-soybean crop rotation system, soybean was planted at Mead site 3 on June 2, 2004. The G/R_n in the beginning of the season was in the range of 0.15 to 0.25 (fig. 10). These values were slightly higher than the values for

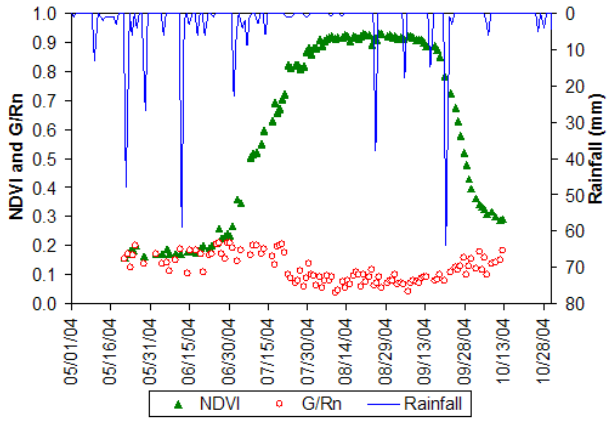

Figure 8. Seasonal progression of G/R_n and NDVI for irrigated soybean at Mead site 2 (maize-soybean rotation) during the crop growing season in 2004. Daily precipitation is also shown in the graph.

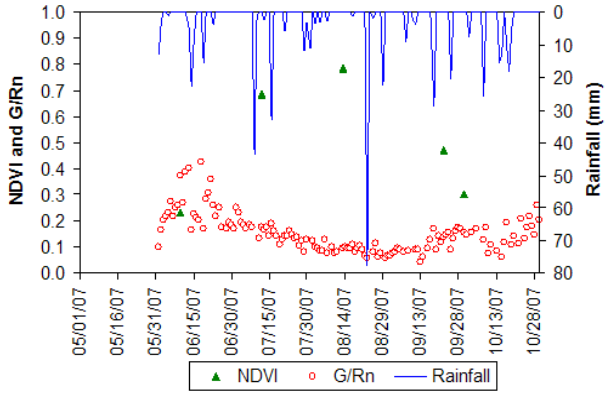

Figure 9. Seasonal progression of G/R_n and NDVI for irrigated soybean at Clay Center during the crop growing season in 2007. Daily precipitation is also shown in the graph.

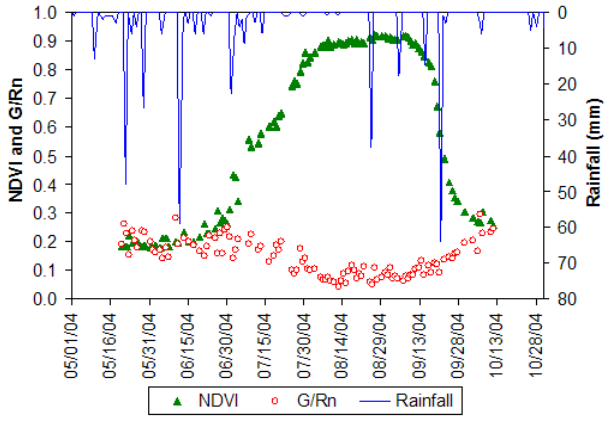

Figure 10. Seasonal progression of G/R_n and NDVI for rainfed soybean at Mead site 3 (maize-soybean rotation) during the crop growing season in 2004. Daily precipitation is also shown in the graph.

irrigated soybeans at Mead site 2 (0.10 to 0.21). The G/R_n ratio at site 3 started to decrease by 36 DAP, reached 0.07 on 64 DAP, and remained fairly uniform in the range of 0.07 to 0.10 during the mid-growing season until 100 DAP. Thereafter, G/R_n started increasing and reached 0.30 by 126 DAP, just 5 days prior to harvesting on October 11, 2004. The NDVI during the mid-growing season remained constant in the range of 0.90 to 0.91. Similar results were obtained by Meyers and Hollinger (2004), who reported that the midday G/R_n for maize and soybean during DOY 200-220 was about 0.08 and 0.065, respectively. They also indicated that for the time period between 6:00 and 12:00 h CST, the average G/R_n was 0.136 for maize and 0.078 for soybean.

Evaluation of the *G* Models under Irrigated and Rainfed Maize Cropping Systems

The statistical comparison of four models for estimating G from measured R_n and NDVI are presented in table 3. The models are listed as M1 (Kustas and Daughtry, 1990), M2 (Bastiaanssen et al., 1998), M3 (Melesse and Nangia, 2005), and M4 (Singh et al., 2008). Predictions from the four models for irrigated maize showed a wide variation from site to site and year to year. At Mead site 1, M2 resulted in the highest MAE (44.1 W m^{-2}) and RMSE (48.6 W m^{-2}) in 2005 (table 3). The lowest values of MAE and RMSE at site 1 using M3 were 17.0 and 24.4 W m^{-2}, respectively, during the 2004 cropping season. Both M2 and M3 resulted in the same r^2 value; however, the higher d (except 2003) and lower MAE and RMSE values of M3 indicated that M3 is a better predictor than M2. Statistically, it is possible to have a high r^2 value and low MAE and RMSE values. Under linear least square regression, r^2 is not a measure of how good the modeled values are, but a measure of how good a predictor can be constructed from the modeled values. The M2 and M3 models have same r^2 value, as both models have same model structure, but they have different regression coefficients. For instance, the regression equation at site 1 in 2003 was $y = 0.897x + 41.85$ for M2, while it was $y = 0.457x + 21.34$ for M3 (table 3).

In general, both M1 and M2 overestimated G at Mead site 1 for all three years, while M3 and M4 underestimated G. Results for Mead site 2 for irrigated maize showed that M2 and M3 yielded the highest (46.7 W m^{-2}) and the lowest (13.5 W m^{-2}) values of MAE, respectively, in 2003. Both models had the same r^2 (0.75), but the d values of M3 was higher than the d obtained with M2 for 2004 and 2005.

The best performance at the Clay Center site for irrigated maize was obtained with M3, with MAE values of 28.6 and 22.2 W m^{-2} for 2005 and 2006, respectively. The corresponding r^2 values were 0.57 and 0.61, respectively. Irrigated maize was grown at the Clay Center site during 2005 and 2006, but the cropping practice in 2007 was irrigated soybean. We should note that Singh et al. (2008) developed M4 by using data from 2005 at the Clay Center site. Therefore, evaluation of M4 for 2005 was excluded from our discussion. The M4 model had the second-lowest MAE and RMSE for 2006 among the four G models. However, its r^2 (0.07) and d (0.52) was very low in 2006.

Rainfed maize was grown at Mead site 3 during 2003 and 2005. The comparison of measured and estimated G for this cropping system showed similar distributions for 2003 and 2005. The M3 model resulted in the lowest MAE during 2003 (10.4 W m^{-2}) and 2005 (9.1 W m^{-2}). In fact, these were the best MAE values achieved among all the cropping systems in our analyses. The highest MAE was obtained using M2, with 49.5 and 53.0 W m^{-2} during 2003 and 2005, respectively. In 2003, the maximum RMSE was 52.9 W m^{-2} (M2) and the minimum RMSE was 15.0 W m^{-2} (M3). The M1 model had the highest correlation during 2003 (r^2 = 0.91) and 2005 (r^2 =

Table 3. Statistical analysis results of the model validations using Kustas and Daughtry (1990) (M1), Bastiaanssen et al. (1998) (M2), Melesse and Nangia (2005) (M3), and Singh et al. (2008) (M4) equations.

		Mead Site 1			Mead Site 2			Mead Site 3			Clay Center		
Statistic	Model[a]	2003	2004	2005	2003	2004	2005	2003	2004	2005	2005	2006	2007
MAE	M1	27.8	34.6	34.6	38.6	34.0	22.7	33.8	27.9	32.8	54.9	57.2	32.1
(W m^{-2})	M2	33.8	42.9	44.1	46.7	27.2	26.3	49.5	27.5	53.0	77.3	70.9	45.3
	M3	23.2	17.0	20.0	13.5	16.7	26.6	10.4	19.3	9.1	28.6	22.2	29.2
	M4	26.8	24.0	30.5	23.9	19.4	31.7	19.7	15.9	18.6	10.1	36.9	31.0
RMSE	M1	30.7	38.0	38.9	41.0	36.2	26.0	34.9	29.4	34.2	57.2	61.2	35.5
(W m^{-2})	M2	39.2	46.3	48.6	50.7	35.2	32.4	52.9	35.2	55.8	81.3	73.1	46.4
	M3	31.7	24.4	27.6	24.7	19.4	35.1	15.0	23.6	17.7	32.1	26.7	50.8
	M4	34.7	31.1	34.6	27.2	22.5	35.6	21.7	18.5	20.5	15.2	43.9	41.2
Slope	M1	0.73	0.66	0.80	0.81	1.16	0.71	0.90	1.05	0.93	0.58	0.54	0.48
	M2	0.90	0.96	1.03	0.91	1.55	0.74	1.05	1.33	0.96	0.39	0.69	0.45
	M3	0.46	0.49	0.53	0.46	0.79	0.38	0.53	0.68	0.49	0.20	0.35	0.23
	M4	0.70	0.69	0.87	1.00	1.24	0.81	0.77	1.05	0.86	0.88	0.35	0.58
Intercept	M1	45.13	57.48	50.27	51.61	24.23	43.14	32.84	26.36	24.60	79.43	82.87	71.61
	M2	41.85	45.79	41.20	53.37	-7.31	45.52	36.87	7.18	41.58	113.2	91.31	93.07
	M3	21.34	23.35	21.01	27.22	-3.73	23.21	18.81	3.66	21.21	57.67	46.57	47.47
	M4	-1.05	3.03	-6.94	-18.27	-27.15	-16.48	-9.91	-16.86	-20.48	15.33	56.06	20.59
r^2	M1	0.76	0.71	0.72	0.82	0.90	0.83	0.91	0.96	0.93	0.94	0.41	0.94
	M2	0.77	0.79	0.78	0.75	0.89	0.69	0.78	0.90	0.81	0.57	0.61	0.88
	M3	0.77	0.79	0.78	0.75	0.89	0.69	0.78	0.90	0.81	0.57	0.61	0.88
	M4	0.62	0.56	0.54	0.77	0.83	0.79	0.89	0.95	0.93	0.88	0.07	0.72
d	M1	0.84	0.74	0.77	0.76	0.78	0.86	0.79	0.85	0.89	0.60	0.46	0.78
	M2	0.81	0.73	0.73	0.70	0.82	0.80	0.63	0.85	0.73	0.44	0.42	0.70
	M3	0.75	0.81	0.79	0.81	0.88	0.64	0.74	0.87	0.72	0.59	0.69	0.52
	M4	0.79	0.98	0.80	0.88	0.90	0.78	0.70	0.93	0.75	0.95	0.52	0.75

[a] M1 = Kustas and Daughtry (1990), M2 = Bastiaanssen et al. (1998), M3 = Melesse and Nangia (2005), and M4 = Singh et al. (2008).

0.93). Similarly, the *d* values were high during these two years (0.79 in 2003 and 0.89 in 2005) for M1. Our results are comparable to other soil heat flux studies. Shao et al. (2008) evaluated the spatial variability in *G* at three steppe ecosystems. They found that the spatial variability of *G* was 48 W m^{-2} (13% of R_n) during the day and 15 W m^{-2} (34% of R_n) at night.

Evaluation of the *G* Models under Irrigated and Rainfed Soybean Cropping Systems

The four models were evaluated for estimating *G* for irrigated and rainfed soybean cropping systems (table 3). The lowest MAE at Mead site 2 was 16.7 W m^{-2} using M3, followed by 19.4 W m^{-2} using M4. The highest MAE at Mead site 2 was obtained using M1 (34.0 W m^{-2}). A very good correlation was obtained at this site for all four *G* models, as indicated by the high r^2 (0.83 to 0.90) and *d* values (0.78 to 0.90). The M3 (0.88) and M4 (0.90) models had very high *d* values, indicating good model performance. Comparison for irrigated soybean at Clay Center during the 2007 cropping season showed that, in general, the MAE and RMSE were higher at this site as compared with Mead site 2 (table 3).

Table 4 shows the PE of MAE and RMSE based on mean measured *G* at the Mead and Clay Center sites. The seasonal average of measured *G* at Mead was considerably higher than at Clay Center. For instance, the mean measured *G* at Mead for the 2005 growing season was 75.7, 97.4, and 102 W m^{-2} for sites 1, 2, and 3, respectively, while it was 39.4 W m^{-2} for the same year at Clay Center (table 4). In 2005, maize was planted at the three Mead sites and at Clay Center. The crops were irrigated at all sites except Mead site 3 (rainfed). The differences in measured *G* between Mead and Clay Center could be attributed to the fact that the soil properties, measurement of *G* (i.e., sensor depth and distance between sensors), irrigation, and residue management conditions were quite different at the sites. For instance, the soil at the Mead sites is silty clay loam, which has about 10% more clay particles than the soil at Clay Center (silt loam). The difference in soil texture will result in variations in soil moisture content, bulk density, and soil temperature between Mead and Clay Center. All of these would ultimately cause variation in thermal soil properties, resulting in variation in soil heat capacity and the diurnal course of *G*. The soil heat flux plates were buried at a depth of 5 cm at the Mead sites, whereas they were placed at a depth of 6 cm at Clay Center. One can argue that the vertical difference in installation depth (1 cm) among the soil heat flux plates is not significant compared to the spatial variation in *G* from soil heat plates buried at the same depth. Shao et al. (2008) reported that the heat storage in the top soil layer accounted for half of the *G* values when the heat flux plate was buried at a depth of 3 cm. At Mead and Clay Center, the soil heat flux plates were installed differently on the crop row. Finally, a major difference among the sites was the residue management. The field at Clay Center was disk-tilled every year, but the three sites at Mead were under no-till conditions (except for disking prior to initiation of the study to homogenize the top 0.10 m of soil in 2001).

Overall, the error for estimating *G* is high for each of the models evaluated at Mead and Clay Center (table 4). Under these high prediction errors, we defined the acceptable *G* estimate as "estimated *G* within an arbitrary 30% of the mean measured value." Based on this criterion, there is no suitable model among all four models evaluated. Although M3 produced slightly better predictions at Mead than the other mod–

Table 4. Percentage errors in validation statistics (MAE and RMSE) for each *G* equation based on mean measured *G* values for each year at Mead and Clay Center, Nebraska.

		Mead Site 1			Mead Site 2			Mead Site 3			Clay Center		
	Model[a]	2003	2004	2005	2003	2004	2005	2003	2004	2005	2005	2006	2007
Measured G[b]		89.9	62.2	75.7	72.3	61.2	97.4	99.5	70.8	102.0	39.4	30.2	52.5
N[c]		128	130	122	122	129	114	131	131	128	184	184	152
MAE	M1	30.9	55.6	45.7	53.4	55.5	23.3	34.0	39.4	32.1	139.2	189.4	61.1
(W m^{-2})	M2	37.6	69.0	58.3	64.6	44.4	27.0	49.7	38.8	51.9	196.0	234.8	86.2
	M3	25.8	27.3	26.4	18.7	27.3	27.3	10.4	27.3	8.9	72.5	73.5	55.6
	M4	29.8	38.6	40.3	33.1	31.7	32.5	19.8	22.5	18.2	25.6	122.2	59.0
RMSE	M1	34.1	61.1	51.4	56.7	59.1	26.7	35.1	41.5	33.5	145.0	202.6	67.6
(W m^{-2})	M2	43.6	74.4	64.2	70.2	57.5	33.3	53.1	49.7	54.7	206.1	242.1	88.3
	M3	35.2	39.2	36.5	34.2	31.7	36.0	15.1	33.3	17.3	81.4	88.4	96.7
	M4	38.6	50.0	45.7	37.6	36.7	36.6	21.8	26.1	20.1	38.5	145.4	78.4

[a] M1 = Kustas and Daughtry (1990), M2 = Bastiaanssen et al. (1998), M3 = Melesse and Nangia (2005), and M4 = Singh et al. (2008).
[b] *G* values represent the seasonal average from May through end of October for a given site and year.
[c] *N* is the number of measurements for each site and year during the growing season (May through end of October).

els, the predictions at Clay Center were poor. These results indicate that while empirical soil heat flux models may produce reasonable estimates of *G* for one site, they do not warrant similar findings for another site. The goodness of fit for each model can be considerably different from site to site and from year to year. This is not unusual, as *G* varies spatially because of the spatial variation in soil properties, vegetation cover, and management conditions. Moreover, the diurnal course of *G* may change from day to day due to variation in the weather (Verhoef et al., 1996) and measurement errors (Liebethal et al., 2005).

The considerable variations in the performance of the models may be attributed to various factors, including soil properties; measurement of G, R_n, and NDVI; and tillage and residue management conditions. In the case of measurement of *G*, Kustas and Daughtry (1990) reported that the soil heat flux plate was buried at a depth of 5 cm, whereas it was placed at a depth of 6 cm for the study reported by Singh et al. (2008). Hence, it is possible that the extra storage of the heat flux in the soil above the soil heat flux plate can cause differences in model performance. Meyers and Hollinger (2004) discussed the impact of storage terms in the surface energy balance of maize and soybean. They showed that these components, taken together, can be about 15% for maize and 7% for soybean cropping systems. The NDVI for models M1 to M4 was calculated based on bandwidths similar to those of the Landsat satellite. In our study, NDVI was calculated at the Mead sites based on bandwidths similar to MODIS and at Clay Center using Landsat data with coarser resolution. Further, M3 (Melesse and Nangia, 2005) and M4 (Singh et al., 2008) were calibrated with NDVI calculated at the top of the atmosphere. However, in the present study, NDVI was calculated at the top of the surface at the Mead sites. Different methods of tillage and crop residue management can also have an impact on *G*. For instance, soybean following maize is likely to have lower *G* due to the greater presence of maize residue, which has different properties. Azooz et al. (1997) showed that no-till practices can result in colder soil temperatures as compared to conventional moldboard plow tillage. All these differences may be sources of the variation in the performance of the models used in this study. Thus, models utilizing readily available information, but with parameters sensitive to soil thermal properties, might be more suitable to estimate *G*.

Conclusions

We used datasets collected from ongoing large projects at Mead and Clay Center, Nebraska, to investigate seasonal and inter-annual progression of the G/R_n ratio and NDVI to understand how G/R_n dynamics respond to changes in soil, climate, land use, and management conditions for maize and soybean cropping systems. On a seasonal basis, the soil heat flux was about 13.1%, 15.2%, 10.9%, and 12.8% of net radiation for irrigated maize, rainfed maize, irrigated soybean, and rainfed soybean, respectively. The lower soil heat flux in soybean fields as compared with the heat flux in maize fields was due to the higher NDVI of soybean. There were inter-annual differences in G/R_n ratios, and the difference in G/R_n was due to the differences in crop rotation practices. For instance, the G/R_n ratio at the site with maize-soybean rotation, which had a lesser amount of residue, varied from 0.25 to 0.45 early in the growing season in 2003 and 2005, indicating that as much as 20% or more R_n was stored in the ground as compared with the site that had continuous maize with a greater amount of residue.

In general, there were considerable variations in the performances of the four models evaluated, depending on site characteristics, crop, and irrigation conditions. Based on the minimum criterion of estimating *G* within 30% of the mean measured value, none of the models was able to accurately predict *G* (within 30% of the measured values) under these experimental conditions. The differences in the performances of the models were attributed to various factors, such as soil properties, *G* measurement depth, and bandwidth for NDVI, model calibration procedures, and residue management conditions. Thus, local calibration of empirical soil heat flux models is essential for reliable estimates of soil heat flux.

Acknowledgement

The authors thank three anonymous reviewers for their constructive suggestions.

References

Azooz, R. H., B. Lowery, T. C. Daniel, and M. A. Arshad. 1997. Impact of tillage and residue management on soil heat flux. *Agric. Forest Meteorol.* 84(3-4): 207-222.

Bastiaanssen, W. G. M., M. Menenti, R. A. Feddes, and A. A. M. Holtslag. 1998. A remote sensing surface energy balance

algorithm for land (SEBAL): 1. Formulation. *J. Hydrol.* 212-213: 198-212.
Chander, G., and B. Markham. 2003. Revised Landsat-5 TM radiometric calibration procedures and postcalibration dynamic ranges. *IEEE Trans. Geosci. and Remote Sensing* 41(11): 2674-2677.
Choudhury, B. J. 1989. Estimating evaporation and carbon assimilation using infrared temperature data. In *Theory and Applications of Optical Remote Sensing*, 628-690. G. Asrar, ed. New York, N.Y.: Wiley.
Clothier, B. E., K. L. Clawson, P. J. Pinter, M. S. Moran, R. J. Reginato, and R. D. Jackson. 1986. Estimation of soil heat flux from net radiation during the growth of alfalfa. *Agric. Forest Meteorol.* 37(4): 319-329.
Daughtry, C. S. T., W. P. Kustas, M. S. Moran, P. J. Pinter Jr., R. D. Jackson, P. W. Brown, W. D. Nichols, and L. W. Gay. 1990. Spectral estimates of net radiation and soil heat flux. *Remote Sensing Environ.* 32(2-3): 111-124.
Dugas, W. A., R. A. Hicks, and R. P. Gibbens. 1996. Structure and functions of C_3 and C_4 Chihuahuan Desert plane communities: Energy balance components. *J. Arid Environ.* 34(1): 63-79.
Gitelson, A. A., A. Vina, T. J. Arkebauer, D. Rundquist, G. P. Keydan, and B. Leavitt. 2003. Remote estimation of leaf area index and green leaf biomass in maize canopies. *Geophys. Research Letters* 30(5): 52-1-52-4.
Heusinkveld, B. G., A. F. G. Jacobs, A. A. M. Holtslag, and S. M. Berkowicz. 2004. Surface energy balance closure in an arid region: Role of soil heat flux. *Agric. Forest Meteorol.* 122(1-2): 21-37.
Irmak, S. 2010. Nebraska water and energy flux measurement, modeling, and research network (NEBFLUX). *Trans. ASABE* 53(4): 1097-1115.
Irmak, A., and S. Irmak. 2008. Reference and crop evapotranspiration in south central Nebraska: II Measurement and estimation of actual evapotranspiration for corn. *J. Irrig. Drain. Eng.* 134(6): 700-715.
Irmak, S., and D. Mutiibwa. 2009a. On the dynamics of stomatal resistance: Relationships between stomatal behavior and micrometeorological variables and performance of Jarvis-type parameterization. *Trans. ASABE* 52(6): 1923-1939.
Irmak, S., and D. Mutiibwa. 2009b. On the dynamics of evaporative losses from Penman-Monteith with fixed and variable canopy resistance during partial and complete maize canopy. *Trans. ASABE* 52(4): 1139-1153.
Irmak, S., and D. Mutiibwa. 2010. On the dynamics of canopy resistance: Generalized-linear estimation and its relationships with primary micrometeorological variables. *Water Resources Research* 46: W08526, doi:10.1029/2009WR008484.
Irmak, S., D. Mutiibwa, A. Irmak, T. J. Arkebauer, A. Weiss, D. L. Martin, and D. E. Eisenhauer. 2008. On the scaling up leaf stomatal resistance to canopy resistance using photosynthetic photon flux density. *Agric. Forest Meteorol.* 148(6-7): 1034-1044.
Jackson, R. D., M. S. Moran, P. S. Slater, and S. F. Biggar. 1987. Field calibration of reference reflectance panels. *Remote Sensing Environ.* 22(1): 145-158.
Kustas, W. P., and C. S. T. Daughtry. 1990. Estimation of the soil heat flux/net radiation ratio from spectral data. *Agric. Forest Meteorol.* 49(3): 205-223.
Kustas, W. P., J. H. Prueger, J. L. Hatfield, K. Ramalingam, and L. E. Hipps. 2000. Variability in soil heat flux from a mesquite dune site. *Agric. Forest Meteorol.* 103(3): 249-264.
Legates, D. R., and G. J. McCabe. 1999. Evaluating the use of "goodness-of-fit" measures in hydrologic and hydroclimatic model validation. *Water Resources Research* 35(1): 233-241.
Liebethal, C., B. Huwe, and T. Foken. 2005. Sensitivity analysis for two ground heat flux calculation approaches. *Agric. Forest Meteorol.* 132(3-4): 253-262.
Malhi, Y., K. McNaughton, and C. Von Randow. 2004. Low-frequency atmospheric transport and surface flux measurements. In *Handbook of Micrometeorology*, 101-118. X. Lee, W. Massman, and B. Law, eds. Dordrecht, The Netherlands: Kluwer Academic.
Melesse, A. M., and V. Nangia. 2005. Estimation of spatially distributed surface energy fluxes using remotely sensed data for agricultural fields. *Hydrol. Proc.* 19(14): 2653-2670.
Meyers, T. P., and S. E. Hollinger. 2004. An assessment of storage terms in the surface energy balance of maize and soybean. *Agric. Forest Meteorol.* 125(1-2): 105-116.
Moriasi, D. N., J. G. Arnold, M. W. Van Liew, R. L. Bingner, R. D. Harmel, and T. L. Veith. 2007. Model evaluation guidelines for systematic quantification of accuracy in watershed simulations. *Trans. ASABE* 50(3): 885-900.
Murray, T., and A. Verhoef. 2007a. Moving towards a more mechanistic approach in the determination of soil heat flux from remote measurements: I. A universal approach to calculate thermal inertia. *Agric. Forest Meteorol.* 147(1-2): 80-87.
Murray, T., and A. Verhoef. 2007b. Moving towards a more mechanistic approach in the determination of soil heat flux from remote measurements: II. Diurnal shape of soil heat flux. *Agric. Forest Meteorol.* 147(1-2): 88-97.
Neale, C. M. U., W. C. Bausch, and D. F. Heermann. 1989. Development of reflectance-based crop coefficients for maize. *Trans. ASAE* 32(6): 1891-1899.
Rouse, J. W., R. H. Haas, J. A. Schell, and D. W. Deering. 1973. Monitoring the vernal advancement and retrogradation (green wave effect) of natural vegetation. Prog. Rep. RSC 1978-1, NTIS No. E73-106393. College Station, Tex.: Texas A&M University, Remote Sensing Center.
Shao, C., J. Chen, L. Li, W. Xu, S. Chen, T. Gwen, J. Xu, and W. Zhang. 2008. Spatial variability in soil heat flux at three Inner Mongolia steppe ecosystems. *Agric. Forest Meteorol.* 148(10): 1433-1443.
Singh, R. K., and A. Irmak, 2009. Estimation of crop coefficients using satellite remote sensing. *J. Irrig. Drain. Eng.* 135(5): 597-608.
Singh, R. K., A. Irmak, S. Irmak, and D. L. Martin. 2008. Application of SEBAL model for mapping evapotranspiration and estimating surface energy fluxes in south-central Nebraska. *J. Irrig. Drain. Eng.* 134(3): 273-285.
Stannard, D., J. Blanford, W. Kustas, W. Nichols, S. Amer, T. Schmugge, and M. Weltz. 1994. Interpretation of surface flux measurements in heterogeneous terrain during the Monsoon '90 experiment. *Water Resources Res.* 30(5): 1227-1239.
Suyker, A. E., S. B. Verma, G. G. Burba, and T. J. Arkebauer. 2005. Gross primary production and ecosystem respiration of irrigated maize and irrigated soybean during a growing season. *Agric. Forest Meteorol.* 131(3-4): 180-190.
Van Oevelen, P. J. 1991. Determination of the available energy for evapotranspiration with remote sensing. MS thesis. Wageningen, The Netherlands: Agricultural University of Wageningen.
Verhoef, A., B. J. J. M. van den Hurk, A. F. G. Jacobs, and B. G. Heusinkveld. 1996. Thermal soil properties for vineyard (EFEDA-I) and savanna (HAPEX-Sahel) sites. *Agric. Forest Meteorol.* 78(1-2): 1-18.
Verma, S. B., A. Dobermann, K. G. Cassman, D. T. Walters, J. M. Knops, T. J. Arkebauer, A. E. Suyker, G. G. Burba, B. Amos, H. Yang, D. Ginting, K. G. Hubbard, A. A. Gitelson, and E. A. Walter-Shea. 2005. Annual carbon dioxide exchange in irrigated and rainfed maize-based agroecosystems. *Agric. Forest Meteorol.* 131(1-2): 77-96.
Vina, A., A. A. Gitelson, D. Rundquist, G. P. Keydan, B. Leavitt, and J. Schepers. 2004. Monitoring maize phenology with remote sensing. *Agron. J.* 96(4): 1139-1147.
Walter-Shea, E. A., C. J. Hays, M. A. Mesarch, and R. D. Jackson. 1993. An improved goniometer system for calibrating field

reference-reflectance panels. *Remote Sensing Environ.* 43(2): 131-138.
Willmot, C. J. 1981. On the validation of models. *Physical Geography* 2(2): 184-194.
Willmot, C. J. 1984. On the evaluation of model performance in physical geography. In *Spatial Statistics and Models*, 443-460. G. L. Gaile, C. J. Willmot, and D. Reidel, eds. Dordrecht, The Netherlands: D. Reidel.
Wilson, K. B., A. Goldstein, E. Falge, M. Aubinet, D. Baldocchi, P. Berbigier, C. Bernhofer, R. Ceulemans, H. Dolman, C. Field, A. Grelle, A. Ibrom, B. E. Law, A. Kowalski, T. Meyers, J. Moncrieff, R. Monson, W. Oechel, J. Tenhunen, R. Valentini, and S. Verma. 2002. Energy balance closure at FLUXNET sites. *Agric. Forest Meteorol.* 113: 223-243.